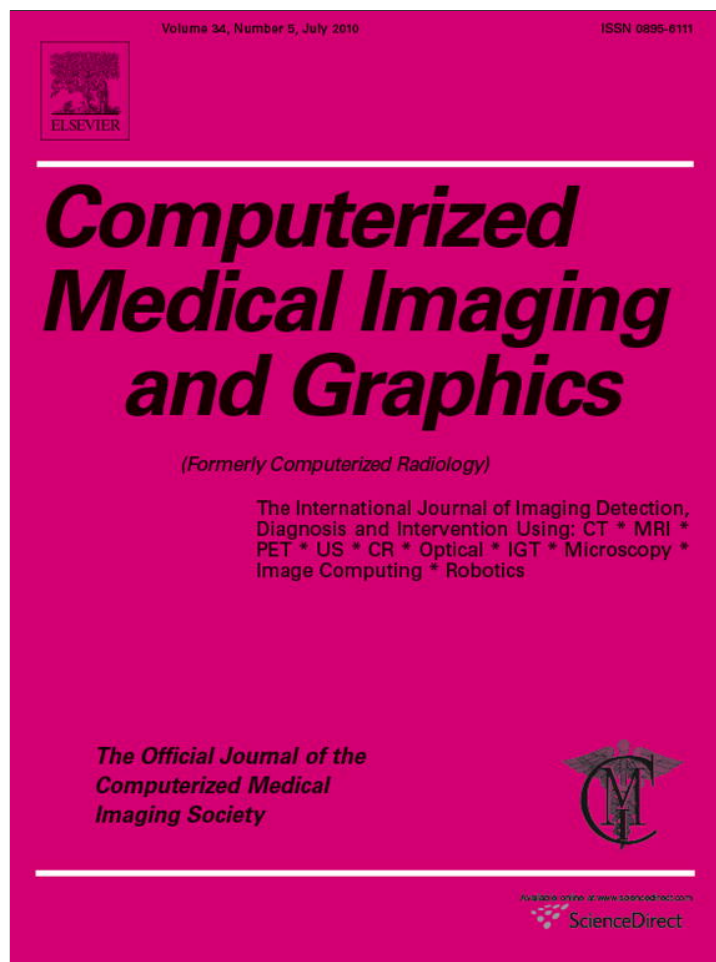


Provided for non-commercial research and education use.
Not for reproduction, distribution or commercial use.



This article appeared in a journal published by Elsevier. The attached copy is furnished to the author for internal non-commercial research and education use, including for instruction at the authors institution and sharing with colleagues.

Other uses, including reproduction and distribution, or selling or licensing copies, or posting to personal, institutional or third party websites are prohibited.

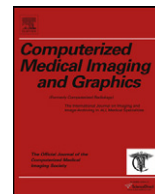
In most cases authors are permitted to post their version of the article (e.g. in Word or Tex form) to their personal website or institutional repository. Authors requiring further information regarding Elsevier's archiving and manuscript policies are encouraged to visit:

<http://www.elsevier.com/copyright>



Contents lists available at ScienceDirect

Computerized Medical Imaging and Graphics

journal homepage: www.elsevier.com/locate/compmedimag

Accuracy of gray-scale coding in lung sound mapping

Atul C. Mehta^{a,1}, Merav Gat^{b,2}, Shlomit Mann^{b,3}, J. Mark Madison^{c,*}^a Pulmonary, Allergy & Critical Care Medicine, Cleveland Clinic, 9500 Euclid Avenue, A90, Cleveland, OH 44195, United States^b Clinical Affairs Department, Deep Breeze, 2 Hailan Street, Or-Akiva, Israel^c Department of Medicine, University of Massachusetts Medical School, University Campus, 55 Lake Avenue North, Worcester, MA 01655, United States

ARTICLE INFO

Article history:

Received 15 January 2009

Received in revised form 6 October 2009

Accepted 14 December 2009

Keywords:

Signal processing

Vibration response imaging

Gray-scale coding

Lung sounds

Respiratory disease

ABSTRACT

Stethoscope evaluation of the lungs is widely accepted and practiced; however, there are some widely recognized, major limitations with its use. A safe device that helped solve these limitations by translating sound into objective, quantifiable images would have clinical utility. Translating lung sounds into quantifiable images in which regional differences or asymmetry in intensities of breath sounds are presented as gradients in gray-scale is not a trivial process. Healthy lungs and lung pathology are characterized by different patterns of regional breath sound distribution and, therefore, the accuracy of mapping gray-scale images must be ensured in a controlled systematic fashion prior to clinical use of such a technique. Vibration response imaging (VRI) maps lung sounds from 40 sensors to a two-dimensional gray-scale image. To assess mapping accuracy, a simulated lung sound map with uniform signals was compared to modified maps where sound signals were reduced (1–3 db) at one sensor. Also, 8 readers evaluated the gray-scale images. The computer algorithm accurately displayed gray-scale coding changes in correct locations in 97% of images. There was $95 \pm 4\%$ accuracy rate by readers to correctly identify gray-scale changes. In addition, quantitative data at different stages of signal processing were investigated in a LSM of a subject with asthma. Signal processing was 97% accurate overall in that the gray-scale values from which the image was derived corresponded with intensity values from recorded signals. These results suggest VRI accurately maps acoustic signals to a gray-scale image and that trained readers can detect small changes.

© 2009 Elsevier Ltd. All rights reserved.

1. Background

Accurate identification of respiratory signs is an important component in the clinical diagnosis of respiratory pathology. The reliability of eliciting physical signs in examination of the chest is relatively poor with 28% of diagnoses being incorrect [1]. Auscultation is a subjective process that is dependant on the auditory acuity and clinical experience of the user and, thus, a quantitative method to obtain reliable information and documentation of lung sounds has been the focus of many investigators.

In the past two decades, computer-based technology has evolved to evaluate the acoustic properties of respiratory sounds and to provide objective measurements that may circumvent the shortcomings of clinical auscultation. A number of studies have

investigated the reliability of acoustic analysis and practical application of this method in clinical diagnosis [2–11]. A multi-national effort was made to establish guidelines on methods of recording and analysis of breath sounds in an attempt to standardize terminology [12].

The display of computerized-based lung sound data varies from graphs of amplitude versus frequency [13], to graphic maps of amplitude contour [14,15], and to gray-scale sound intensity maps [8]. Creating a lung sound map reflecting spatial distribution of sound intensity from a set of signals recorded on a reduced set of spatial coordinates presents the challenge of how to increase spatial resolution without distorting the recorded information. A thorough discussion of approaching this challenge with methods of interpolation has been previously presented [16]. We recently described a new computer-based modality for recording, quantifying, and mapping lung sounds to a two-dimensional gray-scale dynamic and static image [17]. We have termed this modality “vibration response imaging” (VRI). Examples of common characteristics in the normal image, as well as images from patients with various respiratory pathologies have been published [17–24].

As these previous studies with VRI have shown, healthy lungs and lung pathology are characterized by different patterns of regional breath sound distribution on two-dimensional gray-scale

* Corresponding author. Tel.: +1 508 856 6938; fax: +1 508 856 3999.

E-mail addresses: MEHTAA1@ccf.org (A.C. Mehta),

Merav.Gat@deepbreeze.com (M. Gat), Shlomit.Mann@deepbreeze.com (S. Mann),

mark.madison@umassmed.edu (J.M. Madison).

¹ Tel.: +1 216 444 2911; fax: +1 216 445 8160.² Tel.: +972 547 800 259; fax: +972 072 2740023.³ Tel.: +972 547 800 268; fax: +972 072 2740023.

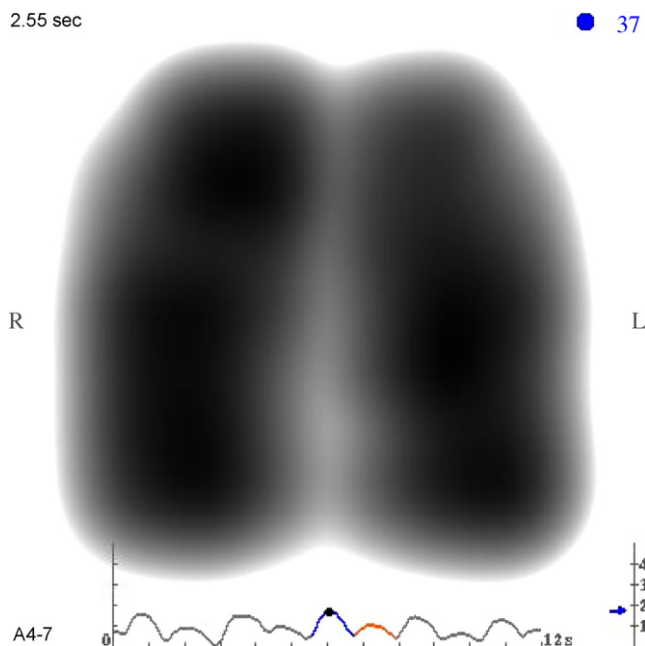


Fig. 1. LSM from a healthy adult male during maximum inspiratory energy. The energy distribution is displayed in the LSM as gray-scale coded values from high vibration energy (black) to minimum (white). A graph of breath sound intensity versus time on a linear time scale is presented under the image. The algorithm selects one respiratory cycle as having the best technical quality (shown here as the 3rd cycle with a blue line for inspiration and a red line for expiration). The dot on the graph indicates the position in the respiratory cycle, and the frame number is given in the upper right-hand corner. (For interpretation of the references to color in this figure legend, the reader is referred to the web version of the article.)

dynamic and static images (Figs. 1 and 2). Translating lung sounds into these quantifiable images in which regional differences or asymmetry in intensities of breath sounds are presented as gradients in gray-scale is not a trivial process. There are 256 degrees of

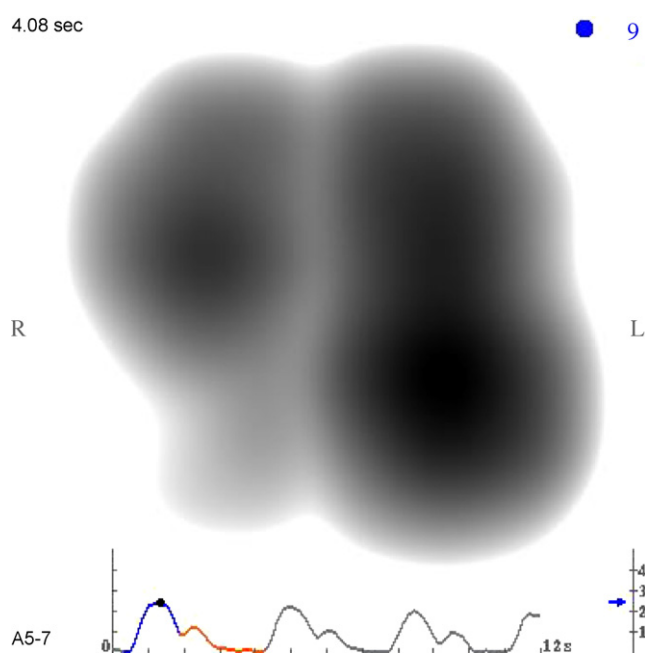


Fig. 2. LSM from an adult female with large right-lung pleural effusion during maximum inspiratory energy. The gray-scale energy distribution on the side of the effusion (right lung) is significantly reduced in the lower lung in comparison with the left lung and with healthy lungs in Fig. 1.

gray-scale coded values that represent a regional distribution pattern for each of the 71 frames in 12 s of recording. Depending on the clinical situation, regional differences or asymmetry in intensities of breath sounds or evidence of adventitious sounds in gray-scale images may prompt, similar to stethoscope use, additional physical examination maneuvers, further diagnostic evaluations (e.g., a chest radiograph), and sometimes treatment. Therefore, the accuracy of mapping acoustic signals to gray-scale images must be ensured in a controlled environment prior to clinical use of such a technique.

The algorithm was designed to take into account the heterogeneity of lung sound distribution and, therefore, if the algorithm is sufficiently robust, then it should demonstrate that even a small decrement of change in adjacent locations can be detected and translated accurately into a quantifiable gray-scale image. Even healthy lungs exhibit some degree of inhomogeneity in lung sound distribution [2,15] and gray-scale images [19,23]. Moreover, this inhomogeneity is emphasized in lung pathology and is reflected in the gray-scale image [18,22].

Given that, the present study was designed to establish the accuracy of the computer algorithm underlying the images created by this system by simulating an environment in which homogeneity of lung sound distribution was absolute and any change in gray-scale distribution was controlled. The first goal was to determine whether small gradients in lung sound intensity were accurately reflected in the displayed image. The second goal was to determine the precision of trained readers to detect these small gradients in gray-scale sound intensity in the images under the best of conditions when the images were purposefully homogeneous. The third goal was to map acoustic signals from a patient with clinical asthma to validate that the intensities of recorded acoustic signals were processed correctly to values for a gray-scale visual image (i.e. louder signals would appear as darker zones in the image based on the gray-scale pixel count values).

2. Methods

2.1. Description of device

The VRIxp™ technology (Deep Breeze™, Or-Akiva, Israel) incorporates 40 active, piezoelectric contact sensors (Meditron ASA, Oslo, Norway) that capture and record lung sounds during the respiration process. The sensors are mounted in two matrices, set in seven rows and three columns (Fig. 3); the two peripheral sensors in the upper row are inactive sensors. The matrices are attached to the posterior chest by a PC-controlled, low vacuum that maintains a constant and simultaneous mechanical load on the sensors. The electrical signals are transmitted through wires from the sensors to the hardware board. The analog signals are then processed by a 64 multi-channels hardware board by amplifying, sampling and A/D conversion (16-bit acquisition level and a sampling rate of 19.2 kHz). The digital data is transmitted to the PC platform where it is processed by the device algorithm and then displayed as a dynamic image.

2.2. Device algorithm

The VRIxp™ technology's algorithm combines the output signals to assemble a gray-scale dynamic image (Fig. 1), or a sequence of lung sound maps (LSM). The gray-scale pattern represents the data signals at each sensor position. N sensors (40 active sensors) are configured for attachment to an essentially planar region, R , on the subject's back [17]. Positions in the region R are designated by two-dimensional position vectors, $x = (x_1, x_2)$. The i sensor ($i = 1$ to N) is fixed at a position x_i in the region R and generates a signal,

denoted herein by $p(xi, t)$ that is indicative of pressure waves in the body arriving at xi . A sound envelope (EVP) is obtained from the signal at each of the N sensors, as follows: the digitized sound signal is band-pass filtered between 150 and 250 Hz in order to select only the desirable frequency range of breath sounds [11] and to reduce other interfering sounds, e.g. heart, muscles, environmental noise, etc. [8]; median filtering is applied to suppresses impulse noise, and then truncation of samples above a pre-defined threshold is performed. Additionally, Singular Value Decomposition is used to detect and extract small signals from noisy data. Then the average vibration energy over a short time interval (frame with duration 0.17 s) is obtained for signals from each of the sensors. Thus, the energy is calculated at each position of the sensors in 71 points along a time scale. For all N sensors, the lower energy threshold is defined as 4% of the maximum value calculated from all $N \times 71$ EVP values.

The energy distribution is displayed in the LSM as 256 degrees of gray-scale coded values from white to black colors. The size of the map is 750×750 pixels. Each of the 562,500 pixels is defined within the gray-scale scheme and combined to create the LSM for each frame of the dynamic image. A column of pixel grids, corresponding with location of the vertebral column, is automatically defined as white. The sensors signals are mapped in 70 pixel intervals in each direction with gray-scale coding from the darkest shade (high data values), in which lung sound is greatest, to white (low data values). The ratio between gray-scale values of different positions in the LSM is dependent on the intensity and location of signals. Each of the sensors has a defined position that corresponds with a specific pixel grid within in the LSM (Fig. 4). High data areas, where breath sound intensity are greatest, are depicted as dark colors (black) within the 256 hues and low data areas are shown in light colors (light gray); the minimum data area is depicted as white. Each subject's recording has different high and low value

	Left				Right		
	1	2	3	4	5	6	7
1							
2							
3							
4							
5							
6							
7							

Fig. 4. Sensor position. The sensors have a defined position (denoted by the numbers in the "x, y"-axes for horizontal and vertical column numbers, respectively) that corresponds with a specific pixel grid within the LSM. The position of the central pixel of each sensor appears in the square that represents that particular sensor.

areas within each respiratory cycle, according to the breath sound intensity. Generally, a breath sound has higher intensity in comparison to any background noise; therefore, these sounds will be the dominating input in the gray-scale distribution. Moreover, the 4% energy threshold eliminates values that generally correspond to noise. A graph of breath sound intensity versus time on a linear time scale is presented under the image (Fig. 1).

2.3. Study design of LSM gray-scale accuracy

The following bench tests were performed under controlled conditions. Lung sounds recorded for 12 s during three respiratory cycles of one healthy volunteer were used to produce a basic signal from the central sensor of the left lung (position 3-2). The sensors have a defined position (denoted by the numbers in the horizontal and vertical columns) that corresponds with a specific pixel grid within the LSM (Fig. 4). The signal was duplicated 40 times, using MATLAB version 7.1 (The MathWorks, Inc., Natick, Massachusetts) in order to simulate a uniform LSM, consisting of 71 frames, from the 40 identical lung sound signals (Fig. 5). Modified LSMs were created by decreasing the sound of the signal by 1, 2, or 3 decibels (dB) in a single sensor (Fig. 6). These decrements are equal to a decrease of 21%, 37% and 50%, respectively. They were selected because they are the minimum changes in sound that the human ear can detect [25]. Thus, three modified LSM intensity subgroups were formed. This process was applied to all 40 sensors; thereby 120 modified LSMs and one uniform LSM were produced for evaluation.

In order to determine if decreases in the intensity of sound signals were reflected in the LSM, modified LSMs were compared with the uniform LSMs. For each LSM, each sensor was assigned a value that was equal to the sum of gray-level values in its corresponding area. Gray-scale value decrements in the pixel grids of each sensor were calculated by multiplying the pixel area of the single sensor grid (70×70 pixels) by the gray-scale value (from 0 to 255). The maximum value of 1,249,500 ($70 \times 70 \times 255$) was computed



Fig. 3. The VRlxp™ system. The device incorporates 40 active, piezoelectric contact sensors that capture and record lung sounds during the respiration process. The sensors are mounted in two matrices, set in seven rows and three columns and are attached to the posterior chest by a PC-controlled, low vacuum. The two peripheral sensors in the upper row are inactive sensors.

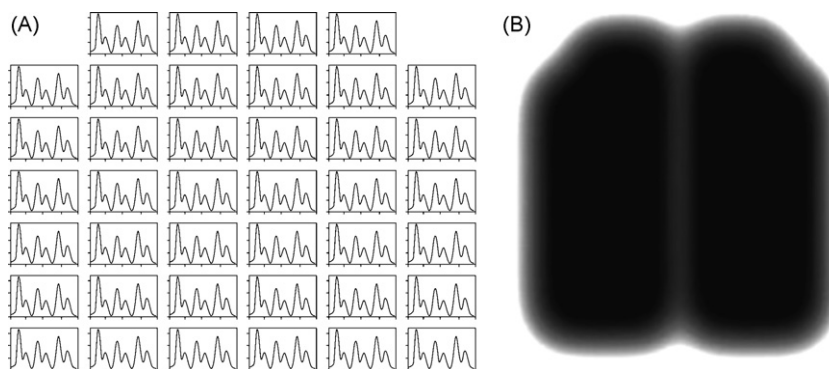


Fig. 5. Simulation process.

(A) A basic signal from the central sensor of the left lung, recorded from a healthy volunteer, was duplicated 40 times. (B) A uniform LSM (frame shown here is at maximum inspiratory energy) was simulated from the 40 identical lung sound signals. The gray-scale coding was uniform in all 562,500 pixels of the LSM.

in order to normalize the values to a range of 0% (no change) to 100% (maximum change) in order to calculate the average gray-level decrement. The level of the change and the location of change were determined for each frame of the LSM in which the change was consistent in the modified sensor. Success was defined as a change of at least one gray-level in the pixels in areas of the modified sensor in all analyzed frames for all the modified LSMs.

The maximum change that occurred in the modified LSM should be observed in the pixel areas corresponding to the sensor that was modified. If this condition exists in at least 96% of the analyzed frames within all 120 modified LSMs then the intensity parameter is validated. This success criterion is due to the inherent boundaries of the dynamic range set forth by the algorithm in order to normalize the gray-scale image. Energy values below the 4% threshold (see Section 2.2) are automatically defined as white and maximum energy values are automatically defined as black in the gray-scale scheme and so changes in intensity in areas of the modified sensor, where the part of it is below the 4% threshold or has maximum value, would not be observed. The LSM success of the algorithm was statistically compared between the three modified LSMs intensity subgroups by *t*-test for paired data, Fisher's exact test and confidence interval (CI).

2.4. Study design for rater evaluation of LSMs

The second phase of the study evaluated the ability of trained, blinded raters to visually detect small gradients in lung sound intensity, represented as gray-scale changes in the LSM. Simulated LSMs were prepared in the same manner as the first phase of the study. A total of 180 LSMs consisting of both uniform ($n = 40$) and modified ($n = 140$) LSMs, were produced for evaluation and randomly presented to the raters. Within the group of 140 LSMs, 20

of the modified LSMs were duplicated for estimating the intra-rater reliability effect. All the evaluations were performed on Eizo screens (FlexScanL557 size 17") with Windows Media Player Classic software.

Eight blinded raters (2 pulmonologists, 3 primary care physicians, and 3 clinical data analysts) were trained to identify intensity changes in the LSM. During the evaluation, the raters examined the dynamic image and then each of the 71 consecutive static frames. The raters then reported if the LSM was modified or uniform. If the LSM was modified, the raters reported the location of the modification (within the upper, middle or lower rows of the right or left lung). All observations were recorded on an evaluation form.

Intra-rater reliability was defined independently for each of the eight raters as the percentage of LSMs that were assessed identically. This analysis set was based on 30 LSMs (20 modified, 10 homogeneous) from the 180 LSMs. Intra-rater reliability was a prerequisite for including the assessments of the raters. Evaluations of raters with less than 80% (allowed maximum: 6 mismatches of 30 LSMs) of intra-rater reliability were not included in the accuracy analysis.

Accuracy analysis was performed on 160 LSMs (40 homogeneous LSMs and 120 modified LSMs; the 20 modified LSMs from the intra-rater reliability analysis were not included). Success was defined as a rater's ability to correctly identify the LSM as homogeneous or modified, and if modified, then to correctly identify the location of the change. The accuracy rate of each rater's assessments is the number of successful evaluations (n_{success}) divided by the number of evaluated LSMs (160). The overall accuracy rate for all eligible raters (maximum eight raters) was calculated as follows:

$$\text{Accuracy Rate} = \frac{\sum_i n_{\text{success}i}}{160 \times i}, \quad i = \text{rater}(1, \dots, 8)$$

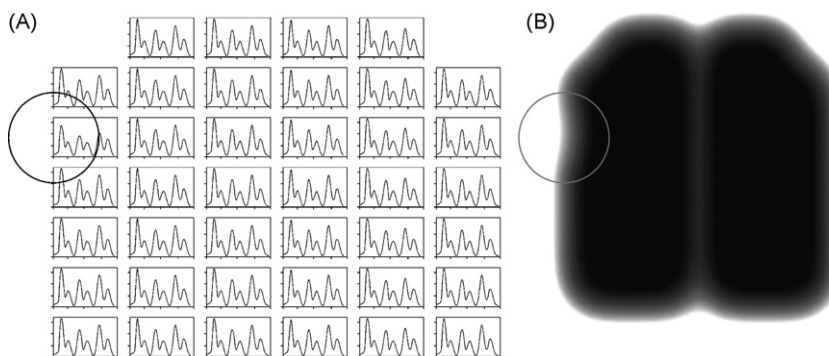


Fig. 6. Modification of the lung sound map.

(A) Signals were decreased by 1 dB in one sensor (position 3.1), as shown by the circled signal set. (B) The gray-scale hue is lighter (decreased signal intensity) in the grid that corresponds with sensor 3.1.

Accuracy parameters were calculated for each rater separately and averaged for all raters (with high intra-rater reliability). Common errors were also investigated in order to determine which parameters had a higher probability for error. The errors were evaluated for the following parameters: intensity mode (decrease or no modification), intensity level (1 dB, 2 dB, or 3 dB), and location (central, outer peripheral, inner peripheral, or corner sensor).

2.5. LSM of subject with lung pathology

In addition to investigating the accuracy of the gray-scale image under controlled conditions (simulated LSMs), another test was performed to validate that the intensities of recorded acoustic signals from a subject with asthma (actual clinical data) were processed correctly to a gray-scale visual image (i.e. louder signals appear as darker zones in the image). Values for the sound envelopes (EVP values) were obtained from the signal at each of the 40 sensors. The gradients (slope) between the EVP value of the analyzed sensor and the EVP values of all its adjacent sensors were tested for each sensor. The signs (positive, negative) of these gradients, before and after algorithm processing, were compared under the assumption that the sign should not be changed.

3. Results

3.1. LSM gray-scale accuracy

The sound signal, which was captured by one central sensor during 12 s of recording, had a noise range of 26.7 db. At the modified sensor, the sound decrements of 1 db, 2 db and 3 db, represented a change of 21%, 37% and 50%, respectively, as compared to the non-modified sensor. After transforming the signal to an LSM, a pixel-by-pixel analysis was performed, in order to assess the performance of the gray-scale algorithm. The uniform LSM showed no gray-level change and had a uniform gray-scale value for the 562,500 pixels. In the modified LSMs, a change of one gray-level or more was detected in the modified sensor in all the analyzed frames.

A maximum gray-level change occurred in a location that corresponded with the location of the intensity modification in all modified 120 LSMs (in at least 96% of the analyzed frames). The change value ranged from 5% (13 gray-levels) to 21% (54 gray-levels). In 78% (94 of 120) of the LSMs, the maximum change was observed at the corresponding modified sensor in all analyzed frames. In 22% (26 of 120) of the LSMs, the maximum change was observed in the modified sensor in 97% of the analyzed frames, and in 3% the maximum change was observed in the sensor adjacent to the modified sensor. This occurred in sensors that are located at the corners (at 10 corner sensors) in frames where a part of the area corresponding to these sensors had a white color because of the dynamic range definition.

As the sound reduction level was modified according to a scale of 0–1 dB (and to 2 dB and 3 dB), the sound decrease rate and percentage of gray-scale absolute change increased (Table 1). A greater decrease in signal intensity resulted in a higher percentage reduc-

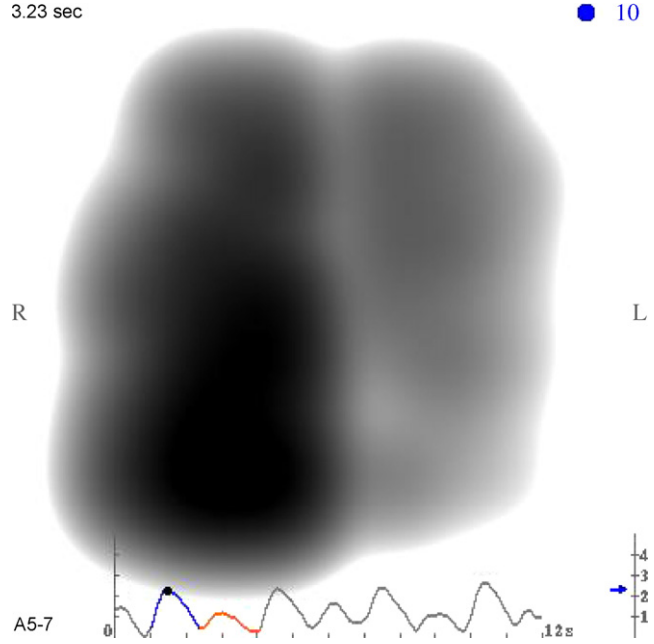


Fig. 7. LSM from an adult male with severe asthma during maximum inspiratory energy. The gray-scale energy distribution shows asymmetries between lungs and irregular distribution within each lung.

tion in gray-scale. The average values for percentage change in the LSMs were $7.1 \pm 1.4\%$, $12.9 \pm 2.2\%$ and $16.4 \pm 3.0\%$ for 1 dB, 2 dB and 3 dB sound modifications, respectively, which are 18.3 ± 3.1 , 32.7 ± 5.8 , 42.0 ± 7.6 in gray-scale units. The differences in observed changes between any two of the three intensity levels (i.e. 1 dB versus 2 dB) were significant ($p < 0.05$, t -test for paired data; see Table 1).

3.1.1. LSM of subject with lung pathology

There were 146 optional comparisons between each of the 40 sensors and adjacent sensors' gradients. The algorithm was 97% (142/146) accurate in processing and translating recorded signals to gray-scale values. Due to the built-in constraints set forth by the dynamic range, values under the lower threshold are set to the actual lower threshold value and would appear white. The regional breath sound distribution in the gray-scale image of the asthmatic patient showed a significantly different mapping pattern (Fig. 7) than a typical pattern in a healthy individual (Fig. 1).

3.2. Rater evaluation of LSMs

The second phase of the study investigated the hypothesis that trained blinded raters had the ability to detect gradients in lung sound intensity, as represented in gray-scale changes in the LSM.

A prerequisite for inclusion in the rater analysis was high intra-rater reliability. The overall intra-rater reliability average for the

Table 1

Sound and pixel change by 0–3 db reductions. As the sound level was reduced in the lung sound maps, according to a scale of 0–1 dB (and to 2 dB and 3 dB), the lung sound intensity was also reduced in the image.

Sound reduction level (db) in sensor(s)	Intensity decrease in gray-scale units (lower, upper 95% confidence intervals)	Intensity decrease in gray-scale (in %) (lower, upper 95% confidence intervals)
0 db decrease	(0, 0)	(0%, 0%)
1 db decrease	(17, 19)	(7%, 8%)
2 db decrease	(31, 35)	(12%, 14%)
3 db decrease	(40, 44)	(15%, 17%)

Table 2

Accuracy statistics per sound intensity change. Overall accuracy rates for the eight raters to correctly identify changes in gray-scale and the location that corresponded with an intensity decrease in one sensor are presented. The error (3 types) represents the sensitivity and specificity of lung sound map assessment.

	1 db decrease	2 db decrease	3 db decrease	Overall decrease
% accuracy	92%	97%	97%	95%
Sensitivity	89%	99%	99%	96%
Specificity	95%	95%	95%	95%

eight raters was $94 \pm 6\%$ (range 83–100%). Seven of the eight raters had an intra-rater reliability of 90–100%. All the raters had high intra-rater reliability and their evaluations were included in the accuracy analysis.

Results were based on evaluation of a total of 1280 LSMs (8 blinded evaluations for 160 LSMs). There was a $95 \pm 4\%$ (1218/1280) overall accuracy rate for the eight raters to correctly identify changes in gray-scale and the location that corresponded with an intensity decrease in one sensor. Error rate per rater ranged from 0% to a maximum of 12.5% (20/160).

Three types of errors were identified: (a) modified LSMs erroneously reported as uniform (3.4%), (b) uniform LSMs that were erroneously reported as modified (1.3%), and (c) inaccurate detection of signal decrease location (0.2%). The error types, (a) and (b), represent the sensitivity (96%) and specificity (95%), respectively, of LSM assessment. The lowest sensitivity (89%) was observed for sound intensity decreases of 1 dB, while greater decreases in sound intensity (2 dB and 3 dB) were more consistently discerned by the raters (sensitivity of 99%) (Table 2). The lowest intensity level (1 dB) resulted in the highest error rate ($p < 0.05$); in contrast, there were no significant differences between 2 dB and 3 dB ($p > 0.05$, Fisher's exact test).

The eight raters had 62 false assessments for the 1280 LSMs that were evaluated. These false assessments occurred in 42 images, representing 42 different combinations of locations and intensity levels. Thirteen images were wrongly assessed by more than one reviewer (Table 3).

The highest rate of evaluation errors occurred for 1 dB decreases in a corner sensor ($n = 16$) and for 1 dB decreases in a central sensor ($n = 14$). These errors accounted for 48% (30/62) of the total evaluation errors in the study. The corner and central sensors had a significantly higher rate of error than the peripheral sensors ($p < 0.05$); there were no significant differences between central and corner sensors ($p > 0.05$, Fisher's exact test).

The accuracy of identifying the location of an LSM intensity change was 99.7% (957/960; 960 = 120 modified LSMs*8 raters). One of the eight raters reported the wrong location of an intensity change in three LSMs. Two location errors were the result of detection of gray-scale decrements in the left lung rather than the right lung; the region (upper, middle or lower) was correctly reported. One location error was made for the upper zone instead of the lower zone, though the lung side was correctly reported.

Table 3

Number of images with false rater assessments. The eight raters had 62 false assessments for the 1280 lung sound maps that were evaluated. These false assessments occurred in 42 images, representing 42 different combinations of locations and intensity levels. Thirteen images were wrongly assessed by more than one reviewer.

False raters' assessment (n)	0 db decrease	1 db decrease	2 db decrease	3 db decrease	Total images (n)
1	12	11	4	2	29
2	2	5	0	1	8
3	0	3	0	0	3
4	0	2	0	0	2
Total images (n)	14	21	4	3	42

4. Discussion

This study shows that the computer algorithm underlying VRI technology is capable of processing recorded sounds into an accurate, two-dimensional, gray-scale map and that trained raters can detect even small decrements in sound displayed in these coded images.

The algorithm was also accurate in processing the intensities of recorded acoustic signals, in the clinical example of an LSM with non-homogenous energy distribution due to asthma (Fig. 7), to a gray-scale visual image (i.e. louder signals appeared as darker zones in the image, as observed in the pixel count values).

These findings validate the foundation of VRI technology and raise the prospect that VRI will ultimately be a sensitive tool for detection and localization of lung pathology that results in even small disturbances in normal respiratory breath sounds.

The aim of this study was to establish the accuracy of the proposed algorithm for gray-scale coding and to evaluate rater accuracy in judging gradients in the gray-scale LSM. A uniform LSM was created by inputting recorded breath sounds from a single sensor into an orderly matrix of 40 sensors. The algorithm then mapped this input into a uniform LSM without changes in gray-level change and with a uniform gray-scale value for the 562,500 pixels. The uniform LSM was then modified by decreasing the input by 1 db, 2 db, or 3 db at one of the 40 sensors, and the resulting modified LSM demonstrated a change of one gray-level or more in at least one sensor. The success criterion was achieved given that a maximum gray-level change occurred in a location that corresponded with the location of the intensity modification in at least 96% of the frames.

While the main goal of the study was to first test the accuracy of the algorithm under controlled conditions, we also investigated the accuracy of the algorithm to map acoustic signals to a gray-scale image based on actual clinical data. The algorithm was 97% accurate in processing and translating recorded signals from an asthmatic subject to gray-scale values. These results establish that the algorithm can accurately image modifications in sound intensity.

The accuracy of reading and interpreting the dynamic LSM is dependent on an observer's ability to visually discern small changes in spatial acoustic signal intensity in the gray-scale image. Therefore, it was important also to test the ability of a trained observer to perceive intensity gray-scale changes, according to location and size in the LSM, which reflect spatial lung sound properties. This task of detecting lung sound intensity changes at 40 locations would be virtually impossible with a traditional stethoscope. The overall accuracy rate for the eight raters to correctly identify changes in gray-scale was very high ($95 \pm 4\%$). The lowest sensitivity (89%) was calculated for intensity decreases at the level of 1 dB, while a higher sensitivity of 99% resulted for decreases at 2 dB and 3 dB. Since this pattern was expected given that a greater decrease in signal intensity results in a higher percentage change in gray-scale ($7.1 \pm 1.4\%$ for 1 dB versus $12.9 \pm 2.2\%$ for 2 dB and $16.4 \pm 3.0\%$ for 3 db), then these results were not surprising. The majority of raters' errors occurred for 1 dB changes in corner and central sensors. It appears that the margin of a 95-pixel perimeter around the image improves the signal-to-noise ratio in the peripheral sensors and

improves clarity of gray-scale gradients, as there were only two errors in identifying gray-scale changes in the outer periphery.

While excellent results were demonstrated by the raters in this study, it is acknowledged that the LSMs were prepared under controlled and optimal conditions. The original signal was derived from an actual recording, in order to simulate conditions that would exist in a clinical setting; however, the remaining signals were duplicated and modified by the software and likely had an optimal signal-to-noise ratio. A slightly lower accuracy rate would be expected if raters identified changes that would occur in more than one sensor from a recording in a clinical setting. Nonetheless, the current results do show that raters are able to visually perceive even 1 db differences in the LSM under optimal conditions.

Due to the inherent limitations of auscultation, more objective methods have been sought to evaluate respiratory sounds. Methods based on computer analysis of acoustic pulmonary signals provide objective measurements based on reproducible data that are analyzed in terms of quantitative parameters. Results of computerized lung sound data are usually presented in various graphic forms such as amplitude versus time, intensity versus frequency or amplitude versus frequency [2,5,15]. Results can also be displayed as a continuous varying signal of power spectra versus time in a three-dimensional coordinate system or as a sonogram representing the plane frequency versus time [8,9]. VRI technology presents breath sounds as a two-dimensional gray-scale dynamic image derived from EVP values across a spatial matrix covering the lung area and across a time period. Thus the VRI technology allows the simultaneous observation of breath sounds captured by 40 sensors in a single dynamic image, as opposed to 40 separate graphs. A visual representation of the lung sound data provided by the VRI has the advantage of displaying the information in a dynamic format as well, thereby, enhancing the value of this data and enabling the observer to also detect timing differences between the different parts of the lung. Currently, we are conducting a study to examine time delay perception by blinded raters. Time delay perception will most likely assist reviewers in detecting respiratory dynamic disturbances and provide new insights into important issues in lung mechanics, such as regional interdependence, airway-parenchyma interactions and parallel inhomogeneity [26].

5. Conclusions

We have demonstrated that the VRI computer algorithm for gray-scale coding of acoustic signals is robust and that even small gradients in the gray-scale image can be evaluated by a trained rater with excellent accuracy. Reviewers were able to distinguish the spatial lung sound characteristic of intensity differences in a 70×70 pixel grid, corresponding to one sensor, in all locations of the image. Furthermore, the clinical example of lung sounds mapped in a subject with lung pathology provides support that the algorithm can accurately process the intensities of recorded acoustic signals to a gray-scale visual image not just from simulated data, but also from actual clinical data. Presently, the VRITM technology is under research for potential clinical applications in order to improve our understanding of the LSM characteristics that are associated with various respiratory diseases.

Conflict of interest

Drs. Mehta and Madison are past recipients of clinical research funding from Deep Breeze for studies related to lung imaging with VRI. Shlomit Mann has received a salary for the past 3 years from Deep Breeze (manufacturer of the VRI device). Merav Gat has received a salary for the past 5 years from Deep Breeze.

Role of the funding source

The study sponsor, Deep Breeze, participated in the study design and collection and analysis of data.

Acknowledgements

We would like to acknowledge our appreciation to the 8 evaluators, who performed blinded evaluation of the data.

References

- [1] Spiteri MA, Cook DG, Clarke SW. Reliability of eliciting physical signs in examination of the chest. *Lancet* 1988;1:873–5.
- [2] Pasterkamp H, Kraman SS, Wodicka GR. Respiratory sounds. Advances beyond the stethoscope. *Am J Respir Crit Care Med* 1997;156:974–7.
- [3] Mahagnah M, Gavriely N. Repeatability of measurements of normal lung sounds. *Am J Respir Crit Care Med* 1994;149:477–81.
- [4] Piirila P, Sovijarvi AR. Crackles: recording, analysis and clinical significance. *Eur Respir J* 1995;8:2139–48.
- [5] Earis JE, Cheetham BMG. Current methods used for computerized respiratory sound analysis. *Eur Respir Rev* 2000;10:586–90.
- [6] Pasterkamp H, Consunji-Araneta R, Oh Y, Holbrow J. Chest surface mapping of lung sounds during methacholine challenge. *Pediatr Pulmonol* 1997;23:21–30.
- [7] Dalmay F, Antonini MT, Marquet P, Menier R. Acoustic properties of the normal chest. *Eur Respir J* 1995;8:1761–9.
- [8] Kompis M, Pasterkamp H, Wodicka GR. Acoustic imaging of the human chest. *Chest* 2001;120:1309–21.
- [9] Sovijarvi AR, Helistö P, Malmberg LP, Kallio K, Paajanen E, Saarinen A, et al. A new versatile PC-based lung sound analyzer with automatic crackle analysis (HeLSA); repeatability of spectral parameters and sound amplitude in healthy subjects. *Technol Health Care* 1998;6:11–22.
- [10] Murphy RL, Vyshedskiy A, Power-Charnitsky VA, Bana DS, Marinelli PM, Wong-Tse A, et al. Automated lung sound analysis in patients with pneumonia. *Respir Care* 2004;49:1490–7.
- [11] Ploy-Song-Sang Y, Martin RR, Ross WR, Loudon RG, Macklem PT. Breath sounds and regional ventilation. *Am Rev Respir Dis* 1977;116:187–99.
- [12] Sovijarvi ARA, Vanderschoot J, Earis JE. Computerized Respiratory Sound Analysis (CORSA): recommended standards for terms and techniques. *ERS Task Force Report. Eur Respir Rev* 2000;10:595–649.
- [13] Gavriely N, Nissan M, Rubin AH, Cugell DW. Spectral characteristics of chest wall breath sounds in normal subjects. *Thorax* 1995;50:1292–300.
- [14] O'Donnell DM, Kraman SS. Vesicular lung sound amplitude mapping by automated flow-gated phonopneumography. *J Appl Physiol* 1982;53:603–9.
- [15] Dosani R, Kraman SS. Lung sound intensity variability in normal men. A contour phonopneumographic study. *Chest* 1983;83:628–31.
- [16] Charlestone-Villalobos S, Cortes-Rubiano S, Gonzalez-Camarena R, Chi-Lem G, Aljama-Corrales T. Respiratory acoustic thoracic imaging (RATHI): assessing deterministic interpolation techniques. *Med Biol Eng Comput* 2004;42:618–26.
- [17] Dellinger RP, Parrillo JE, Kushnir A, Rossi M, Kushnir I. Dynamic visualization of lung sounds with a vibration response device: a case series. *Respiration* 2008;75:60–72.
- [18] Guntupalli KK, Reddy RM, Loutfi RH, Alapat PM, Bandi VD, Hanania NA. Evaluation of obstructive lung disease with vibration response imaging. *J Asthma* 2008;45:903–7.
- [19] Maher TM, Gat M, Allen D, Devaraj A, Wells AU, Geddes DM. Reproducibility of dynamically represented acoustic lung images from healthy individuals. *Thorax* 2008;63:542–8.
- [20] Kramer MR, Raviv Y, Hardoff R, Shteinmatz A, Amital A, Shitrit D. Regional sound distribution analysis in single lung transplant recipients. *J Heart Lung Transplant* 2007;26:1149–54.
- [21] Bentur L, Livnat G, Husein D, Pollack S, Rotschild M. Dynamic visualization of breath sound distribution in suspected foreign body aspiration: a pediatric case series. *J Bronchol* 2007;14:156–61.
- [22] Mor R, Kushnir I, Meyer JJ, Ekstein J, Ben-Dov I. Breath sound distribution images of patients with pneumonia and pleural effusion. *Respir Care* 2007;52:1753–60.
- [23] Yigla M, Gat M, Meyer JJ, Friedman PJ, Maher TM, Madison JM. Vibration response imaging technology in healthy subjects. *AJR Am J Roentgenol* 2008;191:845–52.
- [24] Wang Z, Bartter T, Baumman BM, Abouzgheib W, Chansky ME, Jean S. Asynchrony between left and right lungs in acute asthma. *J Asthma* 2008;45:575–8.
- [25] Schroeder MR, Atal BS. Generalized short-time power spectra and autocorrelation functions. *J Acoust Soc Am* 1962;34:1679–83.
- [26] Simon BA, Christensen GE, Low DA, Reinhardt JM. Computed tomography studies of lung mechanics. *Proc Am Thorac Soc* 2005;2:517–21.

Atul C. Mehta received his medical degree from Municipal Medical College, Gujarat University in India, trained in Internal Medicine at Saint Francis Medical Center and Delaware County Memorial Hospital, and completed fellowship in Pulmonary Medicine at Cleveland Clinic. Dr. Mehta was the founder and president of the American Association for Bronchology. He serves on the editorial boards for several professional journals including the *Journal of Bronchology*, *Lasers in Surgery and*

Medicine and Cleveland Clinic Journal of Medicine. Currently, Dr. Mehta is Vice-Chairman of the Department of Pulmonary and Critical Care Medicine, Head of the Section of Bronchology and acting Medical Director of the Lung Transplant Team at Cleveland Clinic.

Merav Gat holds a Master of Science degree in Applied Mathematics in conjunction with Biomedical Engineering from the Technion – Israel Institute of Technology. She has served as the Director of Clinical Affairs at Deep Breeze Ltd. since 2004. Prior to this, she worked for a global leading company in medical and aesthetic lasers and light-based technology. Merav has 12 years of extensive experience in clinical and regulatory affairs. Her expertise includes strategic leadership in clinical research planning and implementation to meet R&D, regulatory (FDA, EC and SFDA) and worldwide marketing goals.

Shlomit Mann holds a Master of Science degree in statistics and population science from Hebrew University in Jerusalem, Israel. She has served as the statistician at

Deep Breeze Ltd. since 2005. Prior to this, she worked for a global leading company in medical and aesthetic lasers and light-based technology. Shlomit has 9 years of extensive experience in clinical research. Her expertise includes designing clinical research protocols, performing data analysis and preparing clinical study reports to meet R&D, regulatory and worldwide marketing goals.

J. Mark Madison received his medical degree from Harvard Medical School in 1979, trained in Internal Medicine at Barnes Hospital of Washington University, and completed fellowship in Pulmonary Medicine at University of California in San Francisco (UCSF). He served as a member of the faculty at UCSF and then the University of Massachusetts, since 1990, where he has been active in basic research, clinical care, and teaching. Currently, he is the Chief of the Pulmonary, Allergy and Critical Care Medicine Division at the University of Massachusetts.